Weak magnetism for antineutrinos in supernovae

C. J. Horowitz*
Nuclear Theory Center and Department of Physics, Indiana University, Bloomington, Indiana 47405
(Received 14 September 2001; published 11 January 2002)

Weak magnetism increases antineutrino mean free paths in core collapse supernovae. The parity violating interference between axial vector and vector currents makes antineutrino-nucleon cross sections smaller than those for neutrinos. We calculate simple, exact correction factors to include recoil and weak magnetism in supernova simulations. Weak magnetism may significantly increase the neutrino energy flux. We calculate, in a diffusion approximation, an increase of order 15% in the total energy flux for temperatures near 10 MeV. This should raise the neutrino luminosity. Weak magnetism also changes the emitted spectrum of $\overline{\nu_x}$ (with $x=\mu$ or τ) and $\overline{\nu_e}$. We estimate that $\overline{\nu_x}$ will be emitted about 7% hotter than ν_x because $\overline{\nu_x}$ have longer mean free paths. Likewise weak magnetism may increase the $\overline{\nu_e}$ temperature by of order 10%. This increase in temperature coupled with the increase in neutrino luminosity should increase the heating in the low density region outside of the neutrino sphere. This, in turn, could be important for the success of an explosion. It is important to check our results with a full simulation that includes Boltzmann neutrino transport and weak magnetism corrections.

DOI: 10.1103/PhysRevD.65.043001 PACS number(s): 97.60.Bw, 11.30.Er, 26.50.+x

I. INTRODUCTION

Core collapse supernovae are dominated by neutrinos; therefore many supernova properties may depend on the nature of neutrino-nucleon interactions. This provides an opportunity to study characteristic symmetries and features of the standard model weak interactions. Supernovae may provide macroscopic manifestations of charge conjugation [1,2] or parity violation [3–5].

In the laboratory at high energies, antineutrino-nucleon cross sections are systematically smaller than neutrino-nucleon cross sections. This is related to charge conjugation and parity violation in the standard model. Nevertheless, most core collapse supernova simulations still use the *same* lowest order cross section $d\sigma_0/d\Omega$ for both neutrinos and antineutrinos:

$$\frac{d\sigma_0}{d\Omega}=\frac{G^2k^2}{4\pi^2}[c_v^2(1+\cos\theta)+c_a^2(3-\cos\theta)]. \qquad (1)$$

Here k is the (incoming) neutrino energy, θ the scattering angle, and the vector c_v and axial vector c_a coupling constants are listed in Table I.

In this paper, we discuss free space corrections to Eq. (1) from nucleon recoil, weak magnetism, strange quarks and single nucleon form factors. These corrections may be important for supernova simulations because they are present at all densities. In contrast, the density dependent nucleon correlations discussed by [6] and [7] are important only at very high densities, well inside the neutrino sphere.

Electron antineutrinos were detected from supernova 1987A via their capture on protons. Weak magnetism reduces this cross section and impacts the deduced neutron star binding energy and antineutrino temperature. Weak magnetism also changes the rate of antineutrino capture in the neutrino driven wind above a protoneutron star. This may change the electron fraction Y_e (ratio of electrons or protons to baryons) and nucleosynthesis yields in the wind [8,9].

However, to confirm this change in Y_e, one should perform supernova simulations including weak magnetism because this may change the neutrino luminosities and emitted spectra which will also impact Y_e. In this paper, we present simple formulas so that these corrections can be incorporated in simulations. We also give estimates of the change in emitted electron antineutrino spectrum and the differences expected between the spectrum of mu or tau antineutrinos and neutrinos.

The reduction in opacities from recoil and weak magnetism should increase luminosities of both neutrinos and antineutrinos as more energy is transported to the neutrino sphere. This could increase heating behind the shock and more than compensate for the smaller antineutrino absorption cross section. Weak magnetism should also reduce the cooling from positron capture on neutrons further increasing the net heating behind the shock. These changes in heating could make a simulation more likely to explode.

Finally, weak magnetism allows mu and tau antineutrinos to escape the star faster than mu and tau neutrinos. This should lead to a large muon number (number of mu neutrinos minus antineutrinos) or tau number of up to 10^{54} for the hot protoneutron star [1]. This is accompanied by a nonzero chemical potential for mu and tau neutrinos.

Accurate treatments of neutrino transport are now feasible based on the Boltzmann equation [10]. Therefore, it is important to systematically improve neutrino opacities. In Sec. II, we catalog a number of possible opacity corrections.

In Sec. III, we present exact neutrino-nucleon cross sections for both charged and neutral currents. These are accurate to all orders in k/M where k is the neutrino energy and M the nucleon mass. We also present corrections from single nucleon form factors and strange quark contributions in the

*Email address: charlie@iucf.indiana.edu

TABLE I. Coupling constants. Here $g_a \approx 1.260$, $\sin^2\theta_w \approx 0.2325$, $\mu_p = 1.793$ and $\mu_n = -1.913$.

Reaction	c_v	c_a	F_2
$\nu p \to \nu p$	$\frac{1}{2} - 2\sin^2\theta_w \approx 0.035$	$g_a/2 \approx 0.630$	$\frac{1}{2}(\mu_p - \mu_n) - 2\sin^2\theta_w \mu_p \approx 1.019$
$\nu n \to \nu n$	$-\frac{1}{2}$	$-g_a/2 \approx -0.630$	$-\frac{1}{2}(\mu_p - \mu_n) - 2\sin^2\theta_w \mu_n \approx -0.963$
$\left.\begin{matrix}\nu_e n \to e^- p \\ \bar{\nu}_e p \to e^+ n\end{matrix}\right\}$	1	$g_a \approx 1.260$	$\mu_p - \mu_n \approx 3.706$

nucleon. In Sec. IV we discuss recoil and weak magnetism corrections to mu and tau neutrino, energy and lepton number fluxes, and spectra. Section V discusses corrections for electron antineutrinos. We also discuss possible changes in electron fraction Y_e and heating rates. Finally, we conclude in Sec. VI that these weak magnetism and recoil corrections should be incorporated in future supernova simulations.

II. CORRECTIONS TO NEUTRINO OPACITIES

Recently, accurate numerical algorithms have been developed to solve the Boltzmann equation for neutrino transport [10]. The high accuracy of these simulations now warrants systematic improvements in the neutrino opacities. Therefore, we discuss a number of opacity corrections.

The corrections listed in Table II can be divided into two main groups. Numbers 1 through 5 are classified as model independent because they can be calculated exactly and are independent of the model used to describe dense matter. In contrast, corrections 6 through 13 are model dependent. Not only do these corrections depend on the model, but it is important that these corrections be consistent with the equation of state.

Corrections 1, phase space, and 2, matrix element are perhaps the simplest. These are the only ones that are present in the limit of very low densities. They represent more accurate calculations of free space neutrino-nucleon scattering. By phase space we mean corrections from the Q value of the reaction such as the neutron-proton mass difference or because the outgoing neutrino momentum is slightly different from the incoming momentum.

In this paper we focus on number 2, corrections to the matrix element. Recoil corrections, 2a, arise because the nucleon is not infinity heavy and recoils slightly from the neutrino. Weak magnetism, 2b, arises from the parity violating interference between the weak magnetic moment of a nucleon and its axial vector current. Weak magnetism is important because it has opposite sign for neutrinos and antineutrinos. Thus weak magnetism increases the opacity for neutrinos and decreases the opacity for antineutrinos.

The first effects of the dense medium are 3, Pauli blocking of some outgoing nucleon or electron states, and 4, the Fermi or thermal motion of the initial nucleon or electron. These can be calculated exactly. The final model independent correction in Table II is 5, Coulomb corrections. If heavy nuclei are present, the opacity may be dominated by coherent elastic scattering from nuclei. However, these nuclei have strong Coulomb interactions and form a strongly correlated classical liquid. The correlations between ions can greatly reduce the opacity for low energy neutrinos that have wavelengths comparable to the distance between ions. This correction is model independent because the Coulomb interaction is known. For example, Ref. [11] calculated the exact static structure factor of the ions with a simple Monte Carlo simulation. In principle, Coulomb correlations are also present for neutrino electron scattering [12].

Corrections 6–13 depend on the model used for the strong interactions between nucleons. The mean field approximation, 6, is perhaps the simplest way to treat the interactions. Nonrelativistic mean field models incorporate mean field effects in the density of states with an effective mass. Relativistic mean field models have both Lorentz scalar and vector mean fields and the scalar field changes the effective Dirac mass.

It is important that the opacities be consistent with the model used for the equation of state (EOS). This can be achieved by using linear response theory [13] to calculate the response of the medium to a neutrino probe. The random-

TABLE II. Corrections to ν opacities.

	Correction
1.	Phase space
2.	Matrix element
a.	recoil
b.	weak magnetism
c.	form factors
d.	strange quarks
3.	Pauli blocking
4.	Fermi/thermal motion of initial nucleons
5.	Coulomb interactions
6.	Mean field effects
7.	NN Correlations in RPA
8.	NN Correlations beyond RPA
9.	Meson exchange currents
10.	Other components such as hyperons
11.	Other phases such as meson condensates or quark matter
12.	Corrections from superfluid/ superconductor pairing
13.	Nonuniform matter
14.	Magnetic field effects

phase approximation (RPA) or sum of ring diagrams provides the linear response of a mean field theory ground state. Therefore, if one uses a mean field EOS and calculates the opacities in RPA, where the RPA effective interaction is the same as that used for the EOS, then the opacities and EOS will be consistent. For example, the relativistic RPA opacities of Ref. [6] are consistent with their mean field EOS.

We note that the nonrelativistic calculations of Burrows and Sawyer [7] include corrections 1, 3–7 however they do not contain any matrix element correction, 2. Likewise the relativistic RPA calculations of [6] contain corrections 1, 3–7 and 2a recoil but do not contain most of 2b weak magnetism. In the present paper we discuss weak magnetism corrections. In later work we will incorporate these into full nonrelativistic and relativistic RPA calculations.

There are many NN correlations beyond a simple RPA approximation, 8, for example those responsible for $NN \leftrightarrow NN\nu\bar{\nu}$ [15]. In addition there are meson exchange current corrections, 9. The Stony Brook group has done some work calculating corrections from hyperons or other strange hadron components, 10 [18]. More work could be done calculating opacities for meson condensates or other exotic phases of dense matter, 11.

If superfluid or superconducting phases are present there will be pairing corrections to the opacity, 12. These can be important for the late time cooling of a neutron star [16] or perhaps if there is a color superconducting phase [17]. Finally there could be important corrections to opacities in nonuniform matter, 13, for example in the low density pasta phases present in a neutron star inner crust or for a nonuniform meson condensate [14].

All of the above assumed magnetic fields do not play important roles. If magnetic fields are important, they could substantially complicate the opacity, 14, see for example [19]. Magnetic fields might be important in jets or to break the spatial symmetry to explain neutron star kicks [3–5].

To conclude this section, now that accurate neutrino transport is possible, it is important to systematically improve the neutrino opacities. One should include weak magnetism and other free space corrections along with the many density dependent effects. Furthermore, these free space corrections can be included exactly and without any model dependence.

III. NEUTRINO NUCLEON SCATTERING

In this section we discuss recoil, weak magnetism, nucleon form factor, and strange quark corrections to the zeroth order cross section, Eq. (1). Then we present differential, transport and total cross sections that are exact to all orders in the neutrino energy over the nucleon mass k/M.

A. Phase space

Perhaps the simplest correction comes from the phase space of the scattered lepton because its energy k' is less than the incident energy k. If we use full relativistic kinematics for the nucleon and we assume it is originally at rest, then,

$$k' = k/[1+e(1-x)] \equiv \eta k, \tag{2}$$

$$\eta = [1+e(1-x)]^{-1}, \tag{3}$$

with $x = \cos\theta$.

We expect corrections to depend on the small parameter,

$$e \equiv k/M. \tag{4}$$

To the first order in e,

$$k' \approx k[1-e(1-x)]. \tag{5}$$

If one uses the phase space with k' but still uses the matrix element for $M \to \infty$ then Eq. (1) becomes,

$$\frac{d\sigma_{ps}}{d\Omega} = \frac{G^2 k'^2}{4\pi^2}[c_v^2(1+x)+c_a^2(3-x)], \tag{6}$$

$$= \frac{d\sigma_0}{d\Omega}\eta^2, \tag{7}$$

$$\approx \frac{d\sigma_0}{d\Omega}[1-2e(1-x)]. \tag{8}$$

We note that Burrows and Sawyer's work [7] in the limit of low densities reduces to $d\sigma_{ps}/d\Omega$, see Appendix A.

B. Recoil

If one evaluates the matrix element to first order in e and includes the phase space corrections one has,

$$\frac{d\sigma_R}{d\Omega} \approx \frac{d\sigma_0}{d\Omega}[1-3e(1-x)]. \tag{9}$$

We note that the full recoil correction in Eq. (9) is 50% larger than that for $d\sigma_{ps}/d\Omega$ in Eq. (8). Equation (9) still neglects the parity violating interference between axial and vector currents. This interference is dominated by weak magnetism.

C. Weak magnetism

The full weak vector current J_μ has Dirac (c_v) and Pauli or tensor (F_2) contributions,

$$J_\mu = c_v\gamma_\mu + F_2\frac{i\sigma_{\mu\nu}q^\nu}{2M} \tag{10}$$

where $q_\mu = k_\mu - k'_\mu$ is the momentum transfered to the nucleon. The weak current J_μ is related by CVC (conserved vector current) to the electromagnetic current. Therefore the large anomalous magnetic moments of the proton and neutron give rise to a large F_2. The couplings c_v and F_2 are collected in Table I.

The cross section to the first order in e is,

$$\frac{d\sigma}{d\Omega} \approx \frac{d\sigma_0}{d\Omega}\left[1+\left(\pm\frac{4c_a(c_v+F_2)}{c_v^2(1+x)+c_a^2(3-x)}-3\right)e(1-x)\right], \tag{11}$$

with plus sign for ν and minus sign for $\bar{\nu}$. Weak magnetism increases ν and decreases $\bar{\nu}$, while recoil decreases both ν and $\bar{\nu}$ cross sections. Therefore weak magnetism and recoil

corrections approximately cancel for ν but add for $\bar{\nu}$. Note, Burrows *et al.* [20], see also for example [21], include weak magnetism for the charged currents but neglect it for neutral currents. Equation (11) is a good approximation for ν. However it can become negative for large $\bar{\nu}$ energies. To cure this problem we include corrections to all orders in e.

D. Exact cross section

The exact cross section can be calculated, see also [22],

$$\frac{d\sigma}{d\Omega}=\frac{G^2k^2}{4\pi^2}\eta^2\Big\{c_v^2[1+\eta^2-\eta(1-x)] + c_a^2[1+\eta^2+\eta(1-x)]\pm 2c_a(c_v+F_2)(1-\eta^2) + \eta^2\frac{e^2}{2}(1-x)[F_2^2(3-x)+4c_vF_2(1-x)]\Big\}. \quad (12)$$

In general the F_2^2 and c_vF_2 terms are small because they only enter at order e^2. However, their inclusion is important to ensure a positive cross section at high energies. Note, Schinde considers the c_ac_v term but neglected all F_2 contributions [23].

E. Nucleon form factors

The finite size of the nucleon can be included in Eq. (12) by using appropriate form factors,

$$F_2\to F_2(Q^2),\qquad c_v\to c_v(Q^2),\qquad c_a\to c_a(Q^2), \quad (13)$$

that are functions of the four momentum transfer squared,

$$Q^2=-q_\mu^2=2k^2\eta(1-x). \quad (14)$$

For example, for $\nu_e n\to e^- p$,

$$c_a(Q^2)\approx g_a/(1+Q^2/M_A^2)^2, \quad (15)$$

with $g_a\approx 1.26$ and the axial mass $M_A\approx 1$ GeV. Form factors only enter at order e^2. They reduce the cross section by about 10% at $k\approx 100$ MeV, and even less at lower energies. However, for completeness we include simple parametrizations of the form factors in Appendix B. Because the corrections are so small, we will ignore the form factors in the rest of this paper.

F. Total charged current cross section

The opacity for ν_e from charge current reactions depends on the total cross section for $\nu_e n\to e^- p$,

$$\sigma=\int\frac{d\sigma}{d\Omega}d\Omega. \quad (16)$$

The zeroth order result is,

$$\sigma_0=\frac{G^2k^2}{\pi}(c_v^2+3c_a^2), \quad (17)$$

while the correction factor from just phase space is,

$$\sigma_{ps}=\int\frac{d\sigma_{ps}}{\sigma\Omega}d\Omega=\sigma_0R_{ps}(k), \quad (18)$$

$$R_{ps}(k)=\left\{c_v^2\left[\frac{1}{e}-\frac{1}{2e^2}\ln(1+2e)\right]+c_a^2\left[\frac{2e-1}{e(1+2e)}+\frac{1}{2e^2}\ln(1+2e)\right]\right\}\Big/(c_v^2+3c_a^2), \quad (19)$$

$$R_{ps}\approx 1-\frac{4}{3}\left(\frac{c_v^2+5c_a^2}{c_v^2+3c_a^2}\right)e+O(e^2). \quad (20)$$

The exact result is,

$$\sigma=\int\frac{d\sigma}{d\Omega}d\Omega=\sigma_0R(k), \quad (21)$$

$$R(k)=\left\{c_v^2\left(1+4e+\frac{16}{3}e^2\right)+3c_a^2\left(1+\frac{4}{3}e\right)^2 \pm 4(c_v+F_2)c_ae\left(1+\frac{4}{3}e\right)+\frac{8}{3}c_vF_2e^2 + \frac{5}{3}e^2\left(1+\frac{2}{5}e\right)F_2^2\right\}\Big/[(c_v^2+3c_a^2)(1+2e)^3], \quad (22)$$

$$R(k)\approx 1-2\left(\frac{c_v^2+5c_a^2\mp 2(c_v+F_2)c_a}{c_v^2+3c_a^2}\right)e+O(e^2). \quad (23)$$

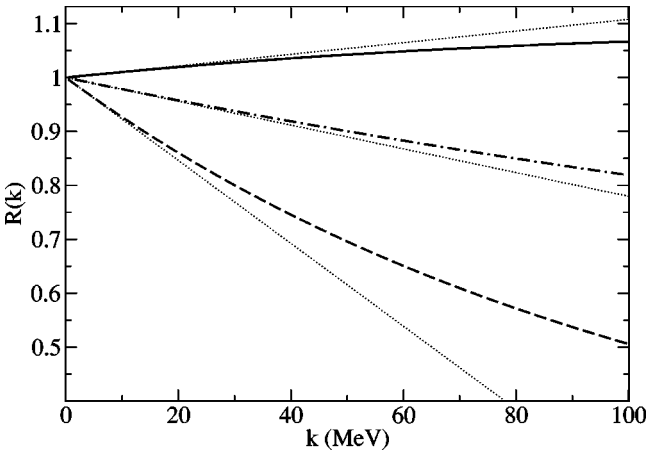

FIG. 1. Factor $R(k)$ that corrects the total charged current cross section for weak magnetism and recoil, Eq. (22), versus neutrino energy k. Solid line is for neutrinos, dashed line is for antineutrinos and the dot-dashed line includes only phase space corrections, Eq. (19). Also shown as dotted lines are the corresponding lowest order correction factors, Eqs. (20) and (23).

For $\bar{\nu}_e$ using Table I this is,

$$R^{-}_{\nu_e} \approx 1 - 7.22e \tag{24}$$

while for ν_e we have,

$$R_{\nu_e} \approx 1 + 1.01e. \tag{25}$$

We note the main effect of weak magnetism and recoil is to reduce the $\bar{\nu}_e$ opacity by the large amount in Eq. (24). For a typical neutrino energy $k \sim \langle E \rangle \sim 20$ MeV this is a 15% reduction.

The full correction factor $R(k)$, is plotted in Fig. 1 along with the lowest order forms in Eqs. (24),(25). We see that the lowest order is fine for neutrinos but fails for antineutrinos above about 50 MeV.

G. Neutral current transport cross section

For mu and tau neutrinos the scattering opacity depends on the transport cross section,

$$\sigma^t = \int d\Omega \frac{d\sigma}{d\Omega}(1-x). \tag{26}$$

Note, strictly speaking this is true only in the limit $k' = k$ nevertheless Eq. (26) provides a good estimate when $k' \approx k$.

The zeroth order transport cross section is

$$\sigma^t_0 = \frac{G^2 k^2}{\pi} \frac{2}{3}(c_v^2 + 5c_a^2). \tag{27}$$

The transport cross section including only phase space corrections is

$$\sigma^t_{ps} = \sigma^t_0 R^t_{ps}(k), \tag{28}$$

$$R^t_{ps}(k) = \left\{ c_v^2 \left[\frac{(1+e)}{e^3} \ln(1+2e) - \frac{2}{e^2} \right] + c_a^2 \left[\frac{2e + (2e^2 - e - 1)\ln(1+2e)}{e^3(1+2e)} \right] \right\} \Bigg/ \left[\frac{2}{3}(c_v^2 + 5c_a^2) \right], \tag{29}$$

$$R^t_{ps} \approx 1 - \left(\frac{2c_v^2 + 14c_a^2}{c_v^2 + 5c_a^2} \right) e + O(e^2). \tag{30}$$

Finally the exact transport cross section is

$$\sigma^t = \sigma^t_0 R^t(k), \tag{31}$$

$$\begin{aligned} R^t(k) = \Bigg\{ & c_v^2 \left[\frac{e-1}{2e^3} \ln(1+2e) + \frac{3 + 12e + 9e^2 - 10e^3}{3e^2(1+2e)^3} \right] + c_a^2 \left[\frac{1+e}{2e^3} \ln(1+2e) - \frac{10e^3 + 27e^2 + 18e + 3}{3e^2(1+2e)^3} \right] \\ & \pm (c_v + F_2) c_a \left[\frac{1}{e^2} \ln(1+2e) - \frac{2 + 10e + \frac{28}{3}e^2}{e(1+2e)^3} \right] + c_v F_2 \left[\frac{1}{e^2} \ln(1+2e) - \frac{2}{3} \left(\frac{3 + 15e + 22e^2}{e(1+2e)^3} \right) \right] \\ & + F_2^2 \left[\frac{1}{4e^2} \ln(1+2e) + \frac{8e^3 - 22e^2 - 15e - 3}{6e(1+2e)^3} \right] \Bigg\} \Bigg/ \left[\frac{2}{3}(c_v^2 + 5c_a^2) \right], \end{aligned} \tag{32}$$

$$R^t \approx 1 + \left(\frac{-(3c_v^2 + 21c_a^2) \pm 8(c_v + F_2)c_a}{c_v^2 + 5c_a^2} \right) e + O(e^2). \tag{33}$$

The full correction, Eq. (32), is plotted in Fig. 2. Corrections for $\nu - n$ are very close to those for $\nu - p$ elastic scattering. We also plot the lowest order result, Eq. (33). This fails for antineutrinos at high energies.

H. Strange quark contributions

Neutrino nucleon elastic scattering is sensitive to possible strange quark contributions in the nucleon. Strange quarks do not contribute to $c_v(Q^2 = 0)$ because the nucleon has no net strangeness. However both $F_2(Q^2 = 0)$ and $c_a(Q^2 = 0)$ can be modified. Parity violating electron scattering constrains F_2 [24]. In this section we concentrate on c_a because F_2 only contributes at order k/M.

Strange quark contributions are assumed to be isoscalar while the dominant contribution to c_a is isovector. Therefore, strange quarks are expected to increase the cross section for $\nu - p$ scattering and decrease that for $\nu - n$. We write,

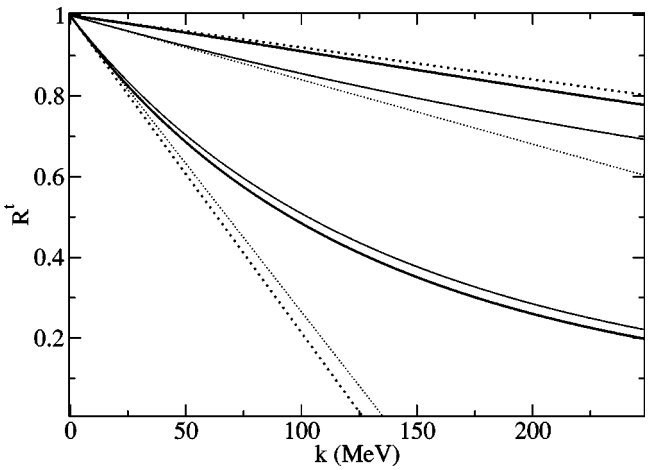

FIG. 2. Factor $R^t(k)$, that corrects transport cross sections for weak magnetism and recoil, Eq. (32), versus neutrino energy k. The upper thick solid line is for $\nu n \to \nu n$ while the upper thin solid line is for $\nu p \to \nu p$. The corresponding lower solid curves are for antineutrino scattering while the dotted curves give lowest order results, Eq. (33).

$$c_a(Q^2=0)=\frac{1}{2}(\pm g_a - g_a^s), \tag{34}$$

with $g_a=1.26$ and the plus sign for $\nu-p$ and the minus sign for $\nu-n$ scattering. The strange quark contribution g_a^s is expected to be negative or zero. The best limit comes from a Brookhaven $\nu-p$ scattering experiment [22]. We assume

$$g_a^s \approx -0.1 \pm 0.1. \tag{35}$$

A better measurement of g_a^s from a laboratory experiment would be very useful.

We make a simple estimate of strange quark effects starting from the zeroth order transport cross section in Eq. (27). We consider the neutral current opacity for a mixture of neutrons and protons of electron fraction Y_e. For simplicity we set $c_v=0$ for $\nu-p$ scattering. The ratio of the opacity with g_a^s to that with $g_a^s=0$ is,

$$S(g_a^s)=\frac{5[g_a^2+(g_a^s)^2]+10g_a g_a^s(1-2Y_e)+1-Y_e}{5g_a^2+1-Y_e}. \tag{36}$$

For $g_a^s=-0.2$, S represents a 21% reduction in the opacity at $Y_e=0.1$ or a 15% reduction at $Y_e=0.2$. Thus strange quarks could reduce opacities by 10–20 %. Note, strange quarks do not contribute to charged current interactions.

IV. MUON AND TAU NEUTRINOS

In this section, we use the weak magnetism and recoil corrections for transport cross sections, Eq. (32) to discuss muon and tau neutrino properties in supernovae. First, we examine muon and tau lepton number currents. Because neutrinos now have shorter mean free paths than antineutrinos, there will be net ν_μ and ν_τ densities and nonzero ν_μ and ν_τ chemical potentials. We then calculate the increase in the ν_μ and ν_τ energy flux because of weak magnetism and recoil. This should increase the neutrino luminosities. Finally we examine corrections to the emitted spectra of ν_μ, ν_τ and $\bar{\nu}_\mu, \bar{\nu}_\tau$. We show that the $\bar{\nu}_\mu, \bar{\nu}_\tau$ are expected to be hotter than ν_μ, ν_τ because of weak magnetism.

For simplicity, we neglect charged muons. These could play some role at very high densities and or temperatures. Without muons, our results are identical for muon and tau neutrinos. Therefore, we write ν_x in this section where x could be μ or τ.

A. Lepton number currents

We start by considering high densities, well inside the neutrino sphere, where a simple diffusion approximation is valid. Earlier work [1,2] calculated the lepton number current to first order in $e=k/m$. We extend this work to all orders.

The transport mean free path for a ν_x of energy k is,

$$\lambda(k)=\lambda_0\frac{k_0^2}{k^2}\frac{1}{R_\nu^t(k)}, \tag{37}$$

with the zeroth order mean free path λ_0 evaluated at an arbitrary reference energy k_0,

$$\lambda_0=[\sigma_0^t(k_0)\rho_n]^{-1}, \tag{38}$$

and ρ_n is the neutron number density. Note, for simplicity we assume pure neutron matter, $Y_e=0$. Because the correction factor R_ν^t, Eq. (32), is so similar for $\nu-p$ and $\nu-n$ scattering our results are not expected to change much for $Y_e>0$.

The lepton number current for ν_x in a simple diffusion approximation is,

$$\vec{J}_{\nu_x}=-\int\frac{d^3k}{(2\pi)^3}\frac{\lambda(k)}{3}\vec{\nabla}\frac{1}{1+\exp[(k-\mu_{\nu_x})/T]}. \tag{39}$$

Here μ_{ν_x} is the neutrino chemical potential. For $\bar{\nu}_x$ we have,

$$\bar{\lambda}(k)=\lambda_0\frac{k_0^2}{k^2}\frac{1}{R_{\bar{\nu}}^t(k)}. \tag{40}$$

This is now longer than $\lambda(k)$ because of the different weak magnetism correction factors $R_{\bar{\nu}}^t < R_\nu^t$. The $\bar{\nu}_x$ lepton number current has the same form as Eq. (39) with μ_{ν_x} replaced by $-\mu_{\nu_x}$,

$$\vec{J}_{\bar{\nu}_x}=-\int\frac{d^3k}{(2\pi)^3}\frac{\bar{\lambda}(k)}{3}\vec{\nabla}\frac{1}{1+\exp[(k+\mu_{\nu_x})/T]}. \tag{41}$$

The total lepton number current is,

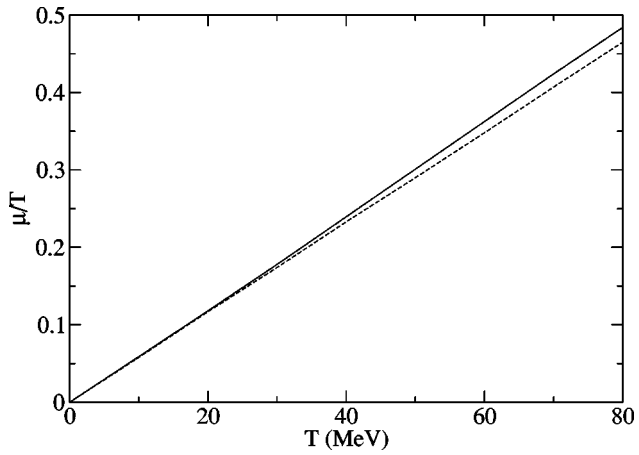

FIG. 3. Muon or tau neutrino chemical potential over temperature μ_{ν_x}/T versus T for matter in steady state equilibrium. The solid line is the full result from the solution to Eq. (43) while the dashed line is correct to lowest order in k/M and μ/T, Eq. (44).

$$\vec{J}=\vec{J}_{\nu_x}-\vec{J}_{\bar{\nu}_x}$$
$$=-\frac{\lambda_0 k_0^2\vec{\nabla}}{6\pi^2}\left[\int_0^\infty\frac{dk}{R_\nu^t}\frac{1}{1+\exp[(k-\mu_{\nu_x})/T]}\right.$$
$$\left.-\int_0^\infty\frac{dk}{R_{\bar{\nu}}^t}\frac{1}{1+\exp[(k+\mu_{\nu_x})/T]}\right]. \quad (42)$$

If $\vec{J}\neq 0$ the lepton number of the star (number of ν_x − number of $\bar{\nu}_x$) will rapidly change. This buildup in lepton number gives rise to a nonzero chemical potential μ_{ν_x}.

Reference [1] argued that the system rapidly reaches steady state equilibrium where $\vec{J}=\vec{J}_{\nu_x}-\vec{J}_{\bar{\nu}_x}=0$. We numerically solve for the chemical potential μ_{ν_x} so that,

$$\int_0^\infty\frac{dk}{R_\nu^t(k)}\frac{1}{1+e^{(k-\mu_{\nu_x})/T}}=\int_0^\infty\frac{dk}{R_{\bar{\nu}}^t(k)}\frac{1}{1+e^{(k+\mu_{\nu_x})/T}}. \quad (43)$$

This is shown in Fig. 3 as a function of T. This chemical potential insures $J=0$.

If we expand Eq. (43) to first order in μ_{ν_x}/T and use $R_\nu^t(k)$ and $R_{\bar{\nu}}^t(k)$ expanded to the first order in k/M one reproduces the lowest order chemical pot μ_0 of Ref. [1],

$$\mu_{\nu_x}\approx\mu_0=\frac{\delta_c\pi^2}{6}\frac{T^2}{M}, \quad (44)$$

with $\delta_c=8(c_v+F_2)c_a/(c_v^2+5c_a^2)\approx 3.30$ for $\nu-n$ scattering. The lowest order μ_0 is seen in Fig. 3 to be an excellent approximation to the exact result even at $T=80$ MeV. Note, this nonzero μ_{ν_x} can lead to muon number (number of ν_μ minus number of $\bar{\nu}_\mu$) or tau number for the protoneutron star as large as 10^{54} [1].

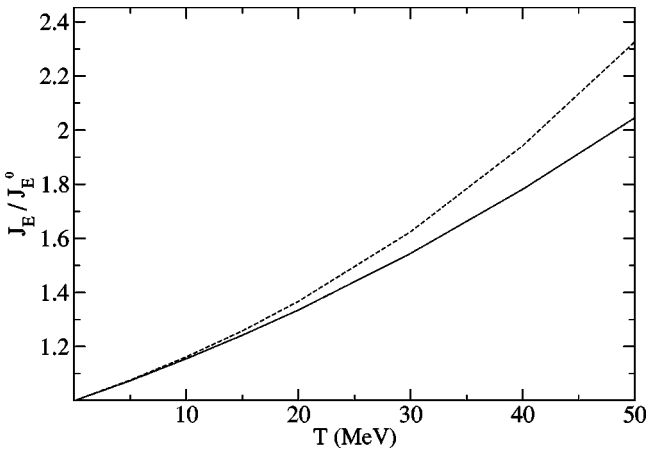

FIG. 4. Ratio of the full energy flux of ν_x and $\bar{\nu}_x$ neutrinos including weak magnetism and recoil J_E to the energy flux without weak magnetism and recoil J_E^0 versus temperature. The solid line is the full result Eq. (46) over Eq. (47). The dashed line neglects the neutrino chemical potential μ_{ν_x} in Eq. (46) and corresponds to $\mu_{\nu_x}=a=0$.

B. Energy flux

We calculate the energy flux carried by ν_x by multiplying the integrand in Eq. (39) by k,

$$\vec{J}_{\nu_x}^E=-\int\frac{d^3k}{(2\pi)^3}\frac{\lambda(k)}{3}\vec{\nabla}\frac{k}{1+e^{(k-\mu_{\nu_x})/T}}. \quad (45)$$

We use Eq. (44) for $\mu_{\nu_x}\approx\mu_0=aT^2$ with $a=\delta_c\pi^2/6M$ and add the $\bar{\nu}_x$ energy flux. We assume the temperature T has only a radial dependence so that,

$$J_E=J_{\nu_x}^E+J_{\bar{\nu}_x}^E$$
$$=-\frac{\lambda_0 k_0^2}{6\pi^2}\frac{dT}{dr}\left[\int_0^\infty\frac{dk}{R_\nu^t}\left(ak+\frac{k^2}{T^2}\right)\right.$$
$$\times(e^{(k/T)-aT}+e^{aT-k/T}+2)^{-1}+\int_0^\infty\frac{dk}{R_{\bar{\nu}}^t}\left(\frac{k^2}{T^2}-ak\right)$$
$$\left.\times(e^{(k/T)+aT}+e^{-aT-k/T}+2)^{-1}\right]. \quad (46)$$

In the absence of weak magnetism and recoil corrections, $\mu_{\nu_x}\equiv 0$ and the energy flux becomes,

$$J_E^0=-\frac{\lambda_0 k_0^2}{6\pi^2}\frac{dT}{dr}2\int_0^\infty dk\frac{k^2}{T^2}(e^{k/T}+e^{-k/T}+2)^{-1}. \quad (47)$$

In Fig. 4 we plot the ratio of the full energy current with weak magnetism and recoil to the zeroth order result J_E/J_E^0. *We see that weak magnetism and recoil substantially enhances the energy flux*. This should raise the neutrino luminosity of the protoneutron star. At a temperature of 30 MeV the enhancement is over 50%.

Many supernova simulations combine ν_x and $\bar{\nu}_x$ into one effective species. In this approximation $\mu_{\nu_x}=0$. Therefore, we evaluate J_E in Eq. (46) while setting $a=0$. This would correspond to using a (geometric) average for the correction factor,

$$\langle R\rangle^{-1}=\frac{1}{2}[(R^t_\nu)^{-1}+(R^t_{\bar{\nu}})^{-1}], \tag{48}$$

for both ν_x and $\bar{\nu}_x$. We see that $J_E(a=0)/J^0_E$ is slightly larger than J_E/J^0_E. This is because the chemical potential somewhat reduces the number of $\bar{\nu}$ and hence their energy current. Even so, $J_E(a=0)$ is a much better approximation than J^0_E.

C. Spectrum

The above lepton number and energy fluxes are based on a diffusion approximation. This is valid inside the neutrino sphere where λ is much less than the size of the system. We now discuss weak magnetism and recoil corrections to the emitted ν_x and $\bar{\nu}_x$ spectra. We will use a simple Monte Carlo model of Raffelt [25] to estimate the emitted spectra. We emphasize that this simple model should be checked against full simulations that include weak magnetism and recoil. Nevertheless, we expect the model to provide a first orientation.

Raffelt [25] discusses the formation of ν_x spectra. At high densities, reactions such as $e^+e^-\leftrightarrow\nu_x\bar{\nu}_x$, $\nu_x e\rightarrow\nu_x e$, or $NN\leftrightarrow NN\nu_x\bar{\nu}_x$ keep ν_x in chemical and thermal equilibrium with the matter. We define the energy sphere as the approximate location where these reactions, which all have small cross sections, become too slow to maintain thermal equilibrium.

Next the ν_x propagate through a scattering atmosphere where neutrinos diffuse because of $N\nu_x\rightarrow N\nu_x$ which has a much larger cross section. However the small energy transfer in nucleon scattering is assumed to be too small to maintain thermal equilibrium. Finally, the neutrinos escape from the neutrino sphere.

Note, the average spectrum for neutrinos and antineutrinos may be modified somewhat by nucleon-nucleon bremsstrahlung in the scattering atmosphere [25]. However, we expect weak magnetism in nucleon scattering to provide an estimate for the *difference* between the spectrum of neutrinos and antineutrinos. This should be explicitly checked in future work that includes weak magnetism for nucleon-nucleon bremsstrahlung.

We model the energy sphere as a blackbody with temperature $T_{ES}\approx 12$ MeV. This high temperature is chosen so that the final temperature of the emitted ν_x agrees with detailed simulations. Alternatively, T_{ES} is the hot matter temperature well inside the neutrino sphere at densities high enough ($\sim 10^{13}$ g cm^3) so that the ν_x are thermalized. We assume the same T_{ES} for both ν_x and $\bar{\nu}_x$ because they are produced in pairs.

We next assume the ν_x propagate through a scattering atmosphere of optical depth,

$$\tau(k)=\frac{\tau_0 k^2}{12T^2_{ES}}R^t_\nu(k). \tag{49}$$

Here τ_0 is the thermally averaged optical depth in the absence of recoil and weak magnetism corrections. Raffelt assumes a Boltzmann distribution for the initial thermalized neutrinos for which $\langle k^2\rangle=12T^2_{ES}$. Note, the optical depth is the thickness of the scattering atmosphere in units of the energy dependent mean free path. A value of $\tau_0\sim 30$ corresponds to one typical simulation [25].

Raffelt calculates the survival probability $S(\tau(k))$ for a ν_x of energy k to make it through the atmosphere and escape. Otherwise it is assumed to be scattered back to the energy sphere and absorbed. A fit to Ref. [25] Monte Carlo results is,

$$S(\tau)=\left[1+\frac{3}{4}\tau\right]^{-1}\times\left[1-\frac{0.033}{1+1.5(l_\tau+0.17)^2+0.5(l_\tau+0.32)^6}\right], \tag{50}$$

with $l_\tau=\log_{10}\tau$. Therefore the final emitted spectrum is,

$$f_{\nu_x}(k)=k^2e^{-k/T_{ES}}S(\tau(k)). \tag{51}$$

For antineutrinos the optical depth is,

$$\bar{\tau}(k)=\frac{\tau_0 k^2}{12T^2_{ES}}R^t_{\bar{\nu}}(k), \tag{52}$$

and the $\bar{\nu}_x$ spectrum is,

$$f^-_{\nu_x}(k)\approx N_0k^2e^{-k/T_{ES}}S(\bar{\tau}(k)). \tag{53}$$

The normalization N_0 is chosen so that $\int_0^\infty dk f^-_{\nu_x}=\int_0^\infty dk f_{\nu_x}$. This corresponds to steady state equilibrium and no net change in the lepton number. Note, N_0 is related to the chemical potential μ_{ν_x}.

The ν_x and the $\bar{\nu}_x$ spectra are shown in Fig. 5. Both of these curves differ from a Boltzmann distribution. Nevertheless the average energy can be characterized by a spectral temperature,

$$T\equiv\langle k\rangle/3. \tag{54}$$

Table III collects T values. We find that T for $\bar{\nu}_x$ is about 7% larger than that for ν_x almost independent of the choice of τ_0. Thus weak magnetism insures that the $\bar{\nu}_x$ spectrum is hotter than that for ν_x. At high energies $R^t_{\bar{\nu}}(k)$ is small. Therefore $f^-_{\bar{\nu}}(k)$ becomes significantly larger than $f_{\nu_x}(k)$. This is shown in Fig. 5 as an increasing ratio of $f^-_{\nu_x}(k)$ to $f_{\nu_x}(k)$. Thus the high energy tail in the spectrum is expected to be antineutrino rich.

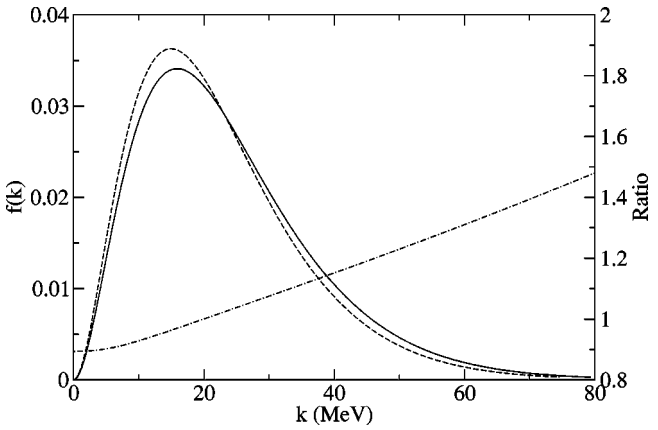

FIG. 5. Spectrum of muon or tau antineutrinos $\bar{\nu}_x$ (solid curve) and neutrinos ν_x (dashed curve) versus neutrino energy k, see Eqs. (51) and (53). The ratio of the $\bar{\nu}_x$ to ν_x spectrum is shown by the dot dashed curve using the right-hand scale.

The difference between the ν_x and the $\bar{\nu}_x$ spectra in Fig. 5 is a macroscopic manifestation of charge conjugation, C, violation in the standard model. If the weak interactions had conserved C then $R^t_\nu = R^t_{\bar{\nu}}$. In principle, this difference is directly observable. However, it may be very difficult to distinguish a detected ν_x from a $\bar{\nu}_x$. Instead, a superposition of the ν_x and the $\bar{\nu}_x$ spectra may be more easily observable. Weak magnetism, by separating the ν_x and the $\bar{\nu}_x$ spectra and by increasing the high energy tail of the $\bar{\nu}_x$ may lead to an observable broadening of the combined ν_x and $\bar{\nu}_x$ spectrum.

V. ELECTRON ANTINEUTRINOS

The reduction in $\bar{\nu}_e$ charged current interactions from weak magnetism and recoil can change the emitted $\bar{\nu}_e$ spectrum, decrease the electron number current and increase the $\bar{\nu}_e$ energy flux. These changes, in turn, impact the Y_e in the neutrino driven wind which is a possible site for r-process nucleosynthesis [8,9]. Finally these changes could be important for analyzing the detected $\bar{\nu}_e$ events from SN 1987A or a future galactic supernova.

A. Lepton number current

The increased $\bar{\nu}_e$ mean free path from recoil and weak magnetism will increase the $\bar{\nu}_e$ number current or decrease the total electron lepton number current $J_e = J_{\nu_e} - J_{\bar{\nu}_e}$. This can increase the ν_e density in the star. For simplicity, consider a situation where μ_{ν_e} is near zero in a simulation without recoil or weak magnetism. Then in steady state equilibrium, we expect recoil and weak magnetism to lead to a μ_{ν_e} of order the μ_{ν_x} from Sec. III, Eq. (44). This chemical potential will lead to an increase in the electron fraction because, in β equilibrium, $\mu_e + \mu_n = \mu_p + \mu_{\nu_e}$. This will lead to a small change in the electron fraction of order,

$$Y_e \sim Y_e^0 \left[1 + \frac{3\mu_{\nu_e}}{\mu_e^0} \right]. \tag{55}$$

Here μ_e^0 is the electron chemical potential and Y_e^0 the electron fraction without weak magnetism and Y_e is the new electron fraction. Using Eq. (44) for μ_{ν_e} at $T = 10$ MeV, $\mu_e^0 = 15$ MeV one has,

$$Y_e \sim Y_e^0 (1 + 0.12) \tag{56}$$

an increase of 10%. Note, Eqs. (55),(56) slightly overestimate the change in Y_e because the charged current opacity for $\bar{\nu}_e$ increases with Y_e. Nevertheless, weak magnetism could lead to a modest increase in Y_e.

In principle, weak magnetism will increase the lepton number diffusion time scale. However this time scale is very sensitive to temperature. We also expect weak magnetism to increase the $\bar{\nu}_e$ energy flux in a similar way to Fig. 4. With weak magnetism, the protoneutron star should cool faster and the lower temperatures will decrease the lepton number diffusion time. These contrary effects should be investigated in a full simulation.

TABLE III. Spectral temperature $T = \langle k \rangle / 3$.

τ_0	T_{ν_x} (MeV)	$T_{\bar{\nu}_x}$ (MeV)	$T_{\bar{\nu}_x}/T_{\nu_x}$
3	8.75	9.24	1.056
10	7.48	7.96	1.064
30	6.49	6.92	1.066
100	5.64	6.04	1.071
300	5.09	5.46	1.073

B. Spectrum of $\bar{\nu}_e$

We consider the following simple model [25] to estimate the change in the $\bar{\nu}_e$ spectrum with weak magnetism. Let the $\bar{\nu}_e$ neutrino sphere be at a temperature T_0 without weak magnetism. For simplicity we assume a Boltzmann spectrum e^{-k/T_0}.

Now we include weak magnetism and recoil described by $R^-_\nu(k)$. This reduction in the opacity will shift the neutrino sphere inwards to higher densities and temperatures. We define a new energy dependent temperature $T(k)$ to include this shift,

$$T(k) \approx \left[\frac{1}{R^-_\nu(k)} \right]^u T_0. \tag{57}$$

Here u is the ratio of temperature to density gradients,

$$u = \frac{d \ln T}{d \ln r} \Big/ \left[\frac{d \ln \rho}{d \ln r} - 1 \right], \tag{58}$$

for the protoneutron star at the neutrino sphere. The extra -1 in the denominator follows because the optical depth involves a path integral from the neutrino sphere to infinity [25]. Realistic values of u could be ~ 0.25 to 0.35 [25].

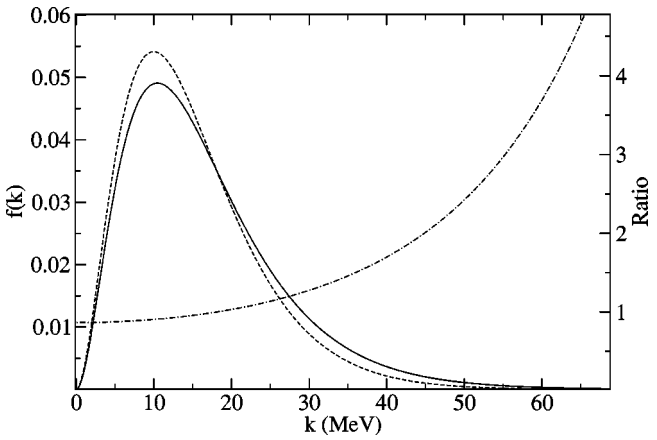

FIG. 6. Spectrum of electron antineutrinos $\bar{\nu}_e$ versus neutrino energy k. The solid curve includes weak magnetism and recoil, Eq. (59), while these are neglected in the dashed curve. The ratio of solid to dashed curves is plotted as the dot-dashed curve using the right-hand scale.

The energy dependent temperature $T(k)$ defines the emitted spectrum

$$f^-_{\nu_e}(k) \approx k^2 e^{-k/T(k)}. \tag{59}$$

If we expand $R^-_\nu(k) \approx 1 - \delta_c k/M$, with $\delta_c = [2c_v^2 + 10c_a^2 + 4(c_v + F_2)c_a]/(c_v^2 + 3c_a^2) + 3 \approx 7.22$ and expand $f^-_{\nu_e}$ to first order in k/M,

$$f^-_{\nu_e}(k) \approx k^2 \left[1 + \frac{u \delta_c k^2}{M T_0} \right] e^{-k/T_0}. \tag{60}$$

We define a spectral temperature $T^-_{\nu_e}$ as,

$$T^-_{\nu_e} \equiv \langle k \rangle / 3 \approx T_0 [1 + 8 u \delta_c T_0 / M]. \tag{61}$$

For $u = 0.3$ and $T_0 = 5$ MeV one has,

$$T^-_{\nu_e} \approx 1.090\, T_0. \tag{62}$$

Thus weak magnetism and recoil can increase the emitted $\bar{\nu}_e$ average energy by of order 10%. It is important to check our simple model with full simulations.

Figure 6 shows the full spectrum, Eq. (60). We see that weak magnetism and recoil shift the strength to higher energies and increase the high energy tail significantly. This is shown by a large ratio of the spectrum with weak magnetism to $k^2 e^{-k/T_0}$ at high energies.

C. Conditions outside the gain radius

We now discuss some possible implications of weak magnetism on neutrino heating, electron fraction and neutrino cooling in the low density region outside the gain radius. The gain radius is the point where cooling from neutrino emission balances heating from neutrino absorption and scattering. The net amount of heating outside the gain radius could be important for the success of the explosion.

The absorption of $\bar{\nu}_e$ outside the gain radius will be reduced by the smaller cross section from weak magnetism. However the cross sections grows with the square of the energy so the new absorption rate may be proportional to,

$$\text{Rate} \sim \left(\frac{T^-_{\nu_e}}{T_0} \right)^2 \langle R^-_{\nu_e}(k) \rangle. \tag{63}$$

The first factor could increase the rate by about 20% while the second factor $\langle R^-_{\nu_e} \rangle \sim 0.8$ could decrease the rate by a similar amount. Therefore, the net rate of $\bar{\nu}_e$ absorption might be little changed. Thus the electron fraction, which depends on the absorption rate, should not change greatly. However, the $\bar{\nu}_e$'s absorbed have a higher energy so the net heating should increase by about 10% because of the higher average energy in Eq. (62).

This assumes the luminosity of the $\bar{\nu}_e$ changed only because of the change in $T^-_{\nu_e}$. If the luminosities of ν_e and $\bar{\nu}_e$ increased further because of the increased energy fluxes in Fig. 4 then the total heating could be even larger.

Finally we discuss cooling from positron capture outside the gain radius,

$$e^+ + p \rightarrow n + \bar{\nu}_e. \tag{64}$$

The rate for Eq. (64) will be reduced by weak magnetism,

$$\begin{aligned} \text{Rate} &\propto \int_0^\infty dk k^2 k^3 R^-_{\nu_e}(k) e^{-k/T}, \\ &\approx \int_0^\infty dk k^5 \left(1 - \delta_c \frac{k}{m} \right) e^{-k/T}, \\ &= 5! T^6 \left(1 - \frac{6 \delta_c T}{M} \right). \end{aligned} \tag{65}$$

At $T = 2$ MeV the factor in parentheses reduces the cooling rate by 9%. Thus weak magnetism can change the $\bar{\nu}_e$ luminosity to increase the heating while, at the same time, reducing the cross section to decrease the cooling. These results should be checked with full simulations.

VI. CONCLUSION

In this paper we examine recoil and weak magnetism corrections to ν-nucleon interactions. These are important because they are present at all densities, even at the relatively low densities near the neutrino sphere. Furthermore, the corrections are model independent. We calculate simple, exact correction factors Eqs. (12),(22),(32) to include recoil and weak magnetism in supernova simulations.

Perhaps the most important effect of weak magnetism and recoil is to increase energy fluxes of both $\bar{\nu}_x$ and $\bar{\nu}_e$ antineutrinos. We calculate, in a diffusion approximation, an increase of order 15% in the total energy flux for temperatures near 10 MeV. This should raise the neutrino luminosity.

Weak magnetism and recoil will also change the emitted

spectrum of $\overline{\nu_x}$ and $\overline{\nu_e}$. We estimate that $\overline{\nu_x}$ will be emitted about 7% hotter than ν_x because $\overline{\nu_x}$ have longer mean free paths. Likewise weak magnetism may increase the $\overline{\nu_e}$ temperature by of order 10%. This increase in temperature coupled with the increase in neutrino luminosity should overcome the reduced absorption cross section and increase the heating in the low density region outside of the neutrino sphere. This, in turn, could be important for the success of an explosion.

We find large corrections. However, supernova simulations are very complicated with many degrees of feedback. Therefore, it is important to check our results with a full simulation that includes Boltzmann neutrino transport and weak magnetism corrections.

ACKNOWLEDGMENTS

We thank John Beacom, Hans-Thomas Janka and Georg Raffelt for extensive discussions of the physics. We thank the Institute for Nuclear Theory in Seattle for its hospitality when this work was started and acknowledge financial support from DOE grant DE-FG02-87ER40365.

APPENDIX A: LOW DENSITY LIMIT OF BURROWS AND SAWYER

In this appendix we discuss the low density limit of Burrows and Sawyer's calculations [7] and show that it reduces to our phase space result, $d\sigma_{ps}/d\Omega$, in Eq. (6). Burrows and Sawyer start by considering a pure vector interaction. Their Eq. (2) for the differential rate of neutrino scattering $\mathbf{k}\rightarrow\mathbf{k}'$ is,

$$\frac{d^2\Gamma}{d\omega d\cos\theta}=\frac{G^2}{4\pi^2}k'^2[1-f_\nu(k')]\Lambda^{00}S(q,\omega). \quad \text{(A1)}$$

Here the momentum transferred to the neutrons is $\mathbf{q}=\mathbf{k}-\mathbf{k}'$ and the energy transferred is $\omega=k-k'$. The neutrino distribution is $f_\nu(k)$ and Λ^{00} is the neutrino tensor, Eq. (3) of Ref. [7]. The dynamic structure function $S(q,\omega)$ for the neutrons is,

$$S(q,\omega)=2\int\frac{d^3p}{(2\pi)^3}f(p)[1-f(|\mathbf{p}+\mathbf{q}|)] \times 2\pi\delta(\omega+\epsilon_p-\epsilon_{p+q}), \quad \text{(A2)}$$

where $f(p)$ is the neutron distribution function and ϵ_p the energy of a neutron of momentum p.

One can recover our Eq. (6) by, (a) neglecting the final state neutrino Pauli blocking, (b) integrating Eq. (A1) over ω, (c) assuming that the density is low enough so that $1-f(\mathbf{p}+\mathbf{q})\approx 1$ in Eq. (A2),

$$\int_0^\infty d\omega S(q,\omega)\approx 2\int\frac{d^3p}{(2\pi)^3}f(p)2\pi, \quad \text{(A3)}$$

$$=2\pi\rho_n. \quad \text{(A4)}$$

Here ρ_n is the neutron density. Finally (d) we assume, in the limit of low density, that the ω dependence of $S(q,\omega)$ is sharply peaked near, $\omega=k-k'$, with k' given by our Eq. (2). Adding a similar expression for the axial interactions gives,

$$\int_0^\infty\frac{d\Gamma}{d\omega d\cos\theta}d\omega\rightarrow 2\pi\rho_n\frac{d\sigma_{ps}}{d\Omega}, \quad \text{(A5)}$$

with $d\sigma_{ps}/d\Omega$ given by our Eq. (6).

APPENDIX B: SINGLE NUCLEON FORM FACTORS

In this appendix we collect simple parametrizations of the single nucleon form factors for use in Eq. (13). We write the weak form factors in terms of the electromagnetic Dirac, F_1^i, and Pauli, F_2^i, form factors for $i=p$ or n.

(i) Reaction $\nu p\rightarrow\nu p$:

$$c_v=\left(\frac{1}{2}-2\sin^2\theta_w\right)F_1^{(p)}-\frac{1}{2}F_1^{(n)} \quad \text{(B1)}$$

$$c_a=\frac{g_a}{2}(1+3.53\tau)^{-2} \quad \text{(B2)}$$

$$F_2=\left(\frac{1}{2}-2\sin^2\theta_w\right)F_2^{(p)}-\frac{1}{2}F_2^{(n)}. \quad \text{(B3)}$$

(ii) Reaction to $\nu n\rightarrow\nu n$:

$$c_v=\left(\frac{1}{2}-2\sin^2\theta_w\right)F_1^{(n)}-\frac{1}{2}F_1^{(p)} \quad \text{(B4)}$$

$$c_a=-\frac{g_a}{2}(1+3.53\tau)^{-2} \quad \text{(B5)}$$

$$F_2=\left(\frac{1}{2}-2\sin^2\theta_w\right)F_2^{(n)}-\frac{1}{2}F_2^{(p)}. \quad \text{(B6)}$$

Reaction $\nu_e n\rightarrow e^- p$:

$$c_v=F_1^{(p)}-F_1^{(n)} \quad \text{(B7)}$$

$$c_a=g_a(1+3.53\tau)^{-2} \quad \text{(B8)}$$

$$F_2=F_2^{(p)}-F_2^{(n)}. \quad \text{(B9)}$$

Here, see Eq. (14),

$$\tau=Q^2/4M^2, \quad \text{(B10)}$$

$$F_1^{(p)}=[1+\tau(1+\lambda_p)]G/(1+\tau), \quad \text{(B11)}$$

$$F_2^{(p)}=\lambda_p G/(1+\tau), \quad \text{(B12)}$$

$$F_1^{(n)}\approx\tau\lambda_n(1-\eta)G/(1+\tau), \quad \text{(B13)}$$

$$F_2^{(n)}=\lambda_n(1+\tau\eta)G/(1+\tau), \quad \text{(B14)}$$

with

$$\lambda_p = 1.793, \quad \lambda_n = -1.913, \tag{B15}$$

$$\eta = (1 + 5.6\tau)^{-1}, \tag{B16}$$

and finally,

$$G = (1 + 4.97\tau)^{-2}. \tag{B17}$$

These parametrizations are from Ref. [26].

[1] C. J. Horowitz and Gang Li, Phys. Lett. B **443**, 58 (1998).
[2] C. J. Horowitz and Gang Li, Phys. Rev. D **61**, 063002 (2000).
[3] A. Vilenkin (unpublished); Astrophys. J. **451**, 700 (1995).
[4] C. J. Horowitz and J. Piekarewicz, Nucl. Phys. **A640**, 281 (1998).
[5] Phil Arras and Dong Lai, Phys. Rev. D **60**, 043001 (1999).
[6] Sanjay Reddy, Madappa Prakash, James M. Lattimer, and Jose A. Pons, Phys. Rev. C **59**, 2888 (1999).
[7] A. Burrows and R. F. Sawyer, Phys. Rev. C **58**, 554 (1998); **59**, 510 (1999).
[8] C. J. Horowitz and Gang Li, Phys. Rev. Lett. **82**, 5198 (1999).
[9] C. J. Horowitz, astro-ph/0108113.
[10] See, for example, M. Rampp and H.-T. Janka, Astrophys. J. Lett. **539**, 33 (2000) or M. Liebendorfer, O. E. B. Messer, A. Mezzacappa, and W. R. Hix, astro-ph/0103024.
[11] C. J. Horowitz, Phys. Rev. D **55**, 4577 (1997).
[12] C. J. Horowitz, Phys. Rev. Lett. **66**, 272 (1991).
[13] A. L. Fetter and J. D. Walecka, *Quantum Theory of Many Particle Systems* (McGraw-Hill, New York, 1971), p. 171.
[14] S. Reddy, G. F. Bertsch, and M. Prakash, Phys. Lett. B **475**, 1 (2000).
[15] Steen Hannestad and Georg Raffelt, Astrophys. J. **507**, 339 (1998).
[16] E. G. Flowers, M. Ruderman, and P. G. Sutherland, Astrophys. J. **205**, 541 (1976); A. D. Kaminker, P. Haensel, and D. G. Yakovlev, Astron. Astrophys. **373**, L17 (2001).
[17] Gregory W. Carter and Sanjay Reddy, Phys. Rev. D **62**, 103002 (2000).
[18] Sanjay Reddy, Madappa Prakash, and James M. Lattimer, Phys. Rev. D **58**, 013009 (1998).
[19] Stephen J. Hardy and Markus H. Thoma, Phys. Rev. D **63**, 025014 (2001).
[20] Adam Burrows, Timothy Young, Philip Pinto, Ron Eastman, and Todd A. Tompson, Astrophys. J. **539**, 865 (2000).
[21] P. Vogel and J. F. Beacom, Phys. Rev. D **60**, 053003 (1999).
[22] L. A. Ahrens *et al.*, Phys. Rev. D **35**, 785 (1987).
[23] P. J. Schinde, Astrophys. J., Suppl. Ser. **74**, 249 (1990).
[24] B. Mueller *et al.*, Phys. Rev. Lett. **78**, 3824 (1997); K. A. Aniol *et al.*, *ibid.* **82**, 1096 (1999).
[25] Georg G. Raffelt, Astrophys. J. **561**, 890 (2001).
[26] M. J. Musolf and T. W. Donnelly, Nucl. Phys. **A546**, 509 (1992).